Molecular Therapy
Methods & Clinical Development
Original Article

Efficient generation of liver sinusoidal endothelial-like cells secreting coagulation factor VIII from human induced pluripotent stem cells

Seiji Mitani,[1] Chihiro Hosoda,[1] Yu Onodera,[1] Yoko Takabayashi,[1] Asuka Sakata,[2] Midori Shima,[2] and Kohei Tatsumi[1,2]

[1]Advanced Medical Science of Thrombosis and Hemostasis, Nara Medical University, Kashihara, Nara 634-8521, Japan; [2]Medicinal Biology of Thrombosis and Hemostasis, Nara Medical University, Kashihara, Nara 634-8521, Japan

Liver sinusoidal endothelial cells (LSECs) and LSEC progenitor cells (LPCs) derived from human pluripotent stem cells (PSCs) are expected as valuable cell sources for the development of cell therapy for hemophilia A, a congenital deficiency of coagulation factor VIII (FVIII), as LSECs are responsible for FVIII production. However, there is room for improvement in the efficiency of LSEC and LPC differentiation from human PSCs. In this study, we sought to optimize the method of mesoderm differentiation induction, the initial step of LSEC differentiation from human PSCs, to efficiently induce LSEC-like cells capable of secreting FVIII from human induced pluripotent stem cells (iPSCs). Following optimization of the concentration and stimulation period of CHIR99021 (glycogen synthase kinase 3β inhibitor), bone morphogenetic protein 4, fibroblast growth factor 2, and Activin A in the mesoderm induction step, approximately 65% and 54% of cells differentiated into LPCs and LSEC-like cells, respectively. Furthermore, we observed substantial FVIII protein secretion from LSEC-like cells *in vitro*. In conclusion, we established an efficient method for obtaining LPCs and functional LSEC-like cells from human iPSCs *in vitro*.

INTRODUCTION

Hemophilia A is a congenital hemorrhagic disease caused by the deficiency of coagulation factor VIII (FVIII) activity. The development of curative therapies, including cell therapy, for hemophilia A is highly anticipated. The main cell type responsible for FVIII production *in vivo* is liver sinusoidal endothelial cells (LSECs),[1,2] which constitute the microvessels of the liver. It has been reported that human FVIII antigen was detected in the blood of mice transplanted with human LSECs.[3] However, the use of human LSECs for hemophilia A cell therapy is complicated by the worldwide shortage of donor livers for LSEC isolation.

Recently, Gage et al. reported the therapeutic efficacy of human pluripotent stem cell-derived LSEC progenitor cells (LPCs) ($CD34^+$ venous endothelial cells) for hemophilia A in a mouse model. In their study, transplanted LPCs were differentiated into LSEC-like cells with FVIII-producing capacity in the host liver, ameliorating the diathesis of hemophilia A.[4] This was the proof-of-concept of human pluripotent stem cells (PSCs) (embryonic stem cell [ESC], and induced pluripotent stem cell [iPSC])-derived LPCs and LSEC-like cells as promising cell sources for hemophilia A cell therapy.

Although several differentiation methods for human PSC-LPCs and PSC-LSECs have been reported,[4–6] the differentiation induction efficiency appears to be relatively low, and there is still room for improvement. LPCs and LSECs can be induced from human PSCs via primitive streak and mesodermal cells, which are precursors of LPCs. Previous reports have suggested that mesoderm marker-positive cells could be efficiently induced, but the induction efficiency of LPCs and LSECs from the mesodermal cells seemed to be inefficient. In addition, there are multiple subtypes of mesodermal cells with regards to differentiation trajectory, and their phenotypes are determined through the precise regulation of signaling pathways during differentiation. In the case of LPC differentiation induction from human PSCs, the bone morphogenetic protein (BMP), fibroblast growth factor (FGF), and Activin/nodal signaling pathways are pivotal for PSC differentiation into primitive streak and mesodermal cells.[4] On the other hand, while the WNT/β-catenin signaling pathway has been reported to play an important role in primitive streak and mesodermal cell differentiation from PSCs,[7,8] the importance of the WNT/β-catenin signaling pathway in primitive streak and mesodermal cell induction in terms of LSEC differentiation has not been fully elucidated.[4–6] Hence, we hypothesize that modification of the mesoderm induction method through WNT/β-catenin signaling pathway regulation would be effective in inducing mesodermal cells that can efficiently differentiate into LPCs and LSECs. In previous studies, mesoderm differentiation was performed under three-dimensional (3D)

Received 28 December 2023; accepted 15 October 2024;
https://doi.org/10.1016/j.omtm.2024.101355.

Correspondence: Seiji Mitani, Advanced Medical Science of Thrombosis and Hemostasis, Nara Medical University, Kashihara, Nara 634-8521, Japan.
E-mail: s_mitani@naramed-u.ac.jp
Correspondence: Kohei Tatsumi, Advanced Medical Science of Thrombosis and Hemostasis, Nara Medical University, Kashihara, Nara 634-8521, Japan.
E-mail: ktatsumi@naramed-u.ac.jp

A

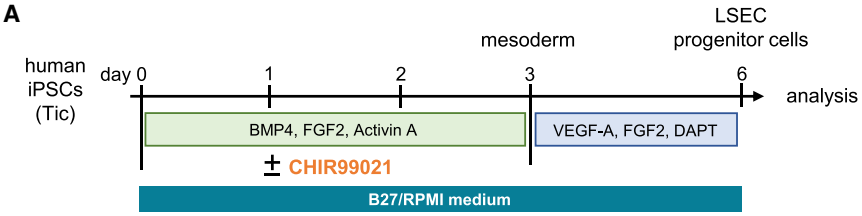

B

Protocol no.	CHIR99021 (μM) day 0–1	day 1–2	day 2–3	note
1	10	5	10	cell detachment was observed on day 3
2	10	5	5	cell detachment was observed on day 3
3	10	5	2	cell detachment was observed on day 6
4	10	5	0	
5	10	10	0	
6	10	2	0	cell detachment was observed on day 6
7	15	5	0	cell death was observed on day 1
8	5	5	0	
9	0	0	0	basic protocol

C

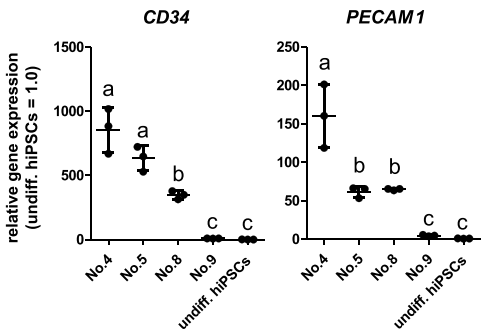

D

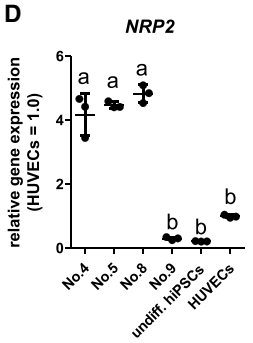

Figure 1. Screening of CHIR99021 treatment condition for the differentiation of LPCs from human iPSCs

(A) Schematic representation of the protocol of human iPSCs (Tic) differentiation into LPCs for the evaluation of the effect of CHIR99021. (B) Details of the CHIR99021 treatment condition. (C) qPCR analysis of *CD34* and *PECAM1* expression in human iPSC derivatives on day 6. On the y axis, expression levels are shown as a relative value to those of undifferentiated human iPSCs. (D) qPCR analysis of *NRP2* gene expression in human iPSC derivatives on day 6. On the y axis, expression levels are shown as a relative value to that of HUVECs. All data are presented as mean ± SD (n = 3). Statistical significance was evaluated by one-way ANOVA followed by Tukey's multiple comparison test. Groups that do not share the same letter above the plots differ significantly from each other ($p < 0.05$). The categorized p values were listed in Table S4. undiff., undifferentiated.

culture conditions after embryo body (EB) formation. However, heterogeneities exist in EBs (e.g., oxygen and nutrient transport, and cellular metabolism)[9] and these heterogeneities in EBs in turn have the possibility of an effect on cell differentiation. Thus, we also hypothesize that a differentiation method under 2D culture conditions is more suitable for the homogeneous differentiation of mesodermal cells compared with the 3D method.

In this study, we attempted to establish an efficient differentiation protocol for LPC and LSEC induction from human iPSCs *in vitro* under 2D culture conditions, with a focus on modulating the primitive streak and mesoderm induction steps. First, we evaluated the effect of WNT/β-catenin signal activation via treatment with glycogen synthase kinase 3β (GSK3β) inhibitor CHIR99021 in the mesoderm induction step on subsequent LPC differentiation. Second, we optimized the stimulation periods of BMP4, FGF2, and Activin A treatment in mesoderm induction. Finally, we differentiated LPCs into LSEC-like cells using the optimized protocol and evaluated their FVIII secretion capacity. By modifying the combination and concentration of CHIR99021, BMP4, FGF2, and Activin A treatment in the primitive streak and mesoderm induction steps, the efficiency of induction of LPCs and LSEC-like cells was significantly improved. Importantly, differentiated LSEC-like cells demonstrated substantial FVIII secretion capacity.

RESULTS

Modification of the mesoderm induction method improved venous CD34$^+$CD31$^+$ cell differentiation efficiency

To improve the differentiation efficiency of human iPSCs into LPCs, we optimized the primitive streak and mesoderm induction steps under 2D culture condition. We first used a human iPSC line called Tic. For optimization, we first evaluated the usefulness of CHIR99021 in the induction of mesodermal cells which could differentiate into LPCs (days 0–3) (Figures 1A and 1B). In the basic protocol (protocol no. 9), we used cytokines (12 ng/mL BMP4, 5 ng/mL FGF2, and 4 ng/mL Activin A) for mesoderm differentiation, as reported previously,[4] by day 3. Based on this protocol, we established an additional eight protocols with different concentrations or stimulation periods of CHIR99021 (protocol nos. 1–8). To induce LPCs, we used cytokines (10 ng/mL FGF2 and 10 ng/mL VEGF-A) and 10 μM DAPT, a notch signaling inhibitor (γ-secretase inhibitor), based on a previous report,[6] on days 3–6 of all differentiation protocols (protocol nos. 1–9). In this step, we used B27/RPMI medium as a basic medium. Differentiation efficiencies were evaluated by qPCR analysis of LPC-related gene expression on day 6. However, the gene expression in cells differentiated using protocol nos. 1, 2, 3, 6, and 7 was not evaluated because these cells had died or detached from the culture plate by day 6. Consequently, the expression of endothelial progenitor cell-related genes (*CD34* and *PECAM1*)[4,6]

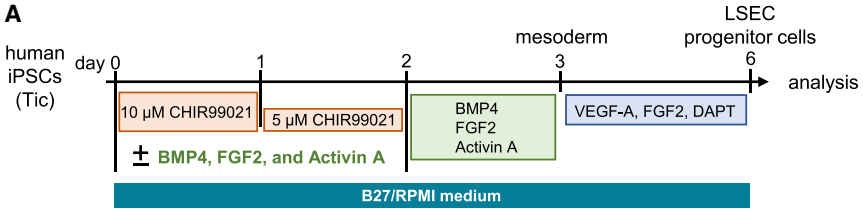

B

Protocol no.	BMP4, FGF2, and Activin A			note
	day 0–1	day 1–2	day 2–3	
4	+	+	+	
10	−	+	+	
11	+	−	+	
12	−	−	+	
9	+ (−CHIR)	+ (−CHIR)	+	basic protocol

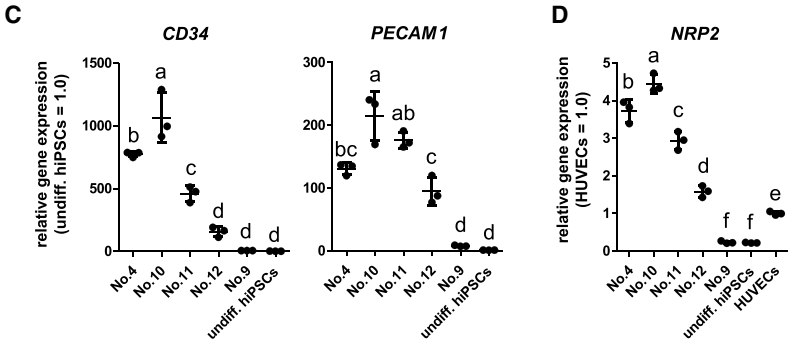

Figure 2. Screening of BMP4, FGF2, and Activin A treatment conditions for the differentiation of LPCs from human iPSCs

(A) Schematic representation of the protocol of human iPSCs differentiation into LPCs for the evaluation of effect of BMP4, FGF2, and Activin A. (B) Detail of the BMP4, FGF2, and Activin A treatment conditions. (C) qPCR analysis of gene (*CD34* and *PECAM1*) expression in human iPSC derivatives on day 6. On the y axis, expression levels are shown as a relative value to those in undifferentiated human iPSCs. (D) qPCR analysis of *NRP2* gene expression in human iPSC derivatives on day 6. On the y axis, the expression levels are shown as a relative value to that of HUVECs. All data are presented as mean ± SD ($n = 3$). Statistical significance was evaluated by one-way ANOVA followed by Tukey's multiple comparison test. Groups that do not share the same letter above the plots differ significantly from each other ($p < 0.05$). The categorized p values are listed in Table S5. undiff., undifferentiated.

in cells induced using protocol no. 4 (treatment with 10 and 5 μM of CHIR99021 on days 0–1 and 1–2, respectively) was higher than that in cells induced using all other protocols (Figure 1C). *CD34* and *PECAM1* gene expression levels in cells induced using protocol no. 4 were approximately 93- and 34-fold higher, respectively, than those induced using protocol no. 9. Moreover, we analyzed the expression of *neuropilin2* (*NRP2*),[10] a venous endothelial cell marker, in human iPSC derivatives, undifferentiated human iPSCs, and human umbilical vein endothelial cells (HUVECs, as a venous endothelial cell control). *NRP2* expression in cells induced using protocol no. 4 was higher than that in cells induced using protocol no. 9, undifferentiated human iPSCs, and HUVECs (Figure 1D).

Next, we evaluated the requirement for BMP4, FGF2, and Activin A in the mesoderm induction step. Based on protocol no. 4, we set additional protocols with different stimulation periods of these additives (protocol nos. 10–12) (Figures 2A and 2B). In this step, we also used B27/RPMI medium as a basic medium. Differentiation efficiencies were evaluated by qPCR analysis of LPC-related gene expression levels on day 6. The gene expression of *CD34*, *PECAM1*, and *NRP2* in cells induced using protocol no. 10 (stimulation with additives during days 1–3) was higher than in cells induced using all other protocols (Figures 2C and 2D). The expression levels of the *CD34* and *PECAM1* genes in cells induced using protocol no. 10 were approximately 1.4- and 1.6-fold higher, respectively, than those induced using protocol no. 4. These results indicated that protocol no. 10 was suitable for the induction of LPCs. Finally, to evaluate the effect of basic medium on differentiation, we performed the differentiation induction using three different base medium conditions (Figure S1A). The expression of *CD34* and *PECAM1* genes in cells induced using protocol no. 10 with B27/RPMI medium was higher than that in cells induced using other conditions (Figure S1B).

In the following, the condition of protocol no. 10 with B27/RPMI medium is referred to as the "modified protocol" (Figure 3A). The percentage of $CD34^+CD31^+$ cells in differentiated cells obtained using the basic and modified protocols was measured using flow cytometry analysis on day 6. Consequently, the percentage of $CD34^+CD31^+$ cells in cells induced using the modified protocol was higher than the basic protocol (approximately 65% vs. 2%) (Figure 3B). In addition, the total number of $CD34^+CD31^+$ cells induced using the modified protocol at day 6 was approximately 4.8-fold greater than the initial cell number at day 0 (Figure 3C).

To examine the characteristics of human iPSC-derived LPCs in detail, we performed magnetic cell sorting (MACS) to isolate $CD34^+$ cells from cells induced using the modified protocol (Figure 3D). Approximately 68% of cells were labeled by CD34 microbeads and they were mostly $CD34^+$ cells (Figures 3E and 3F). Therefore, in the following, cells collected using MACS with CD34 microbeads are referred to as $CD34^+$ cells.

We sought to determine whether cells differentiated using the modified protocol had a venous endothelial phenotype. The gene

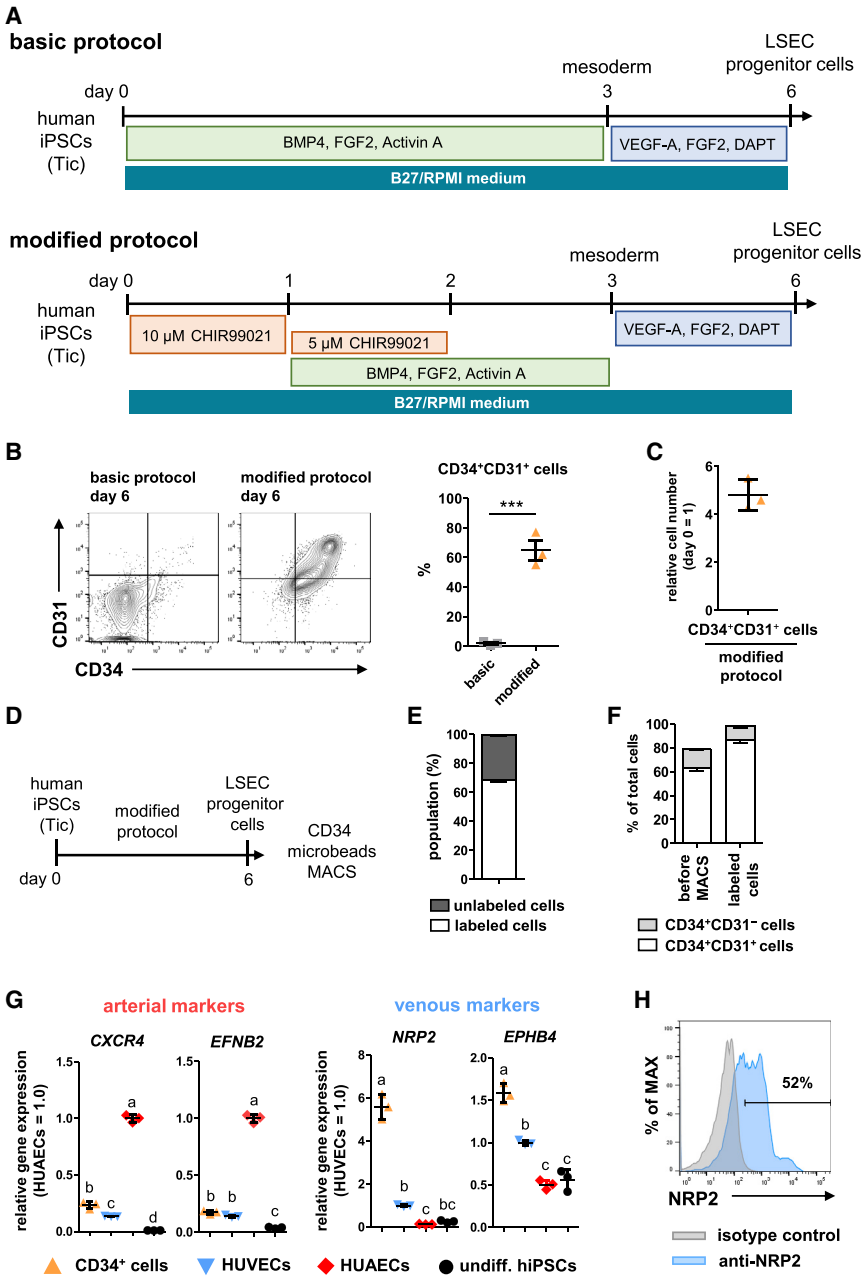

Figure 3. Characterization of human iPSC-derived cells after LPC differentiation induction

(A) Schematic representation of the protocol of human iPSCs (Tic) into LPCs. The basic protocol and our modified protocol are shown. (B) The percentages of $CD34^+$ and $CD31^+$ cells in human iPSC derivatives from the basic and the modified differentiation protocols were measured using flow cytometry analysis. Data are presented as mean ± SEM (n = 3, three independent experiments). Statistically significant differences were evaluated using an unpaired two-tailed Student's t test (***$p < 0.001$). (C) The number of $CD34^+CD31^+$ cells induced using the modified protocol relative to the total cell number at day 0. The number of $CD34^+CD31^+$ cells was calculated from the total cell number and the percentage of $CD34^+CD31^+$ cells measured using flow cytometry on day 6. On the y axis, the total cell number at day 0 taken as 1. Data are presented as mean ± SD (n = 3). (D) Schematic representation of $CD34^+$ cell purification from human iPSC-derived cells. (E) The population of labeled cells and unlabeled cells after MACS. Data are presented as mean −SD (n = 3).

(F) The percentage of $CD34^+$ and $CD31^+$ cells before and after MACS was measured using flow cytometry. Data are presented as mean −SD (n = 3). (G) qPCR analysis of *CXCR4*, *EFNB2*, *NRP2*, and *EPHB4* expression in $CD34^+$ cells collected from human iPSC derivatives induced by the modified protocol. For *CXCR4* and *EFNB2*, on the y axis, expression levels are shown as a relative value to those in HUAECs. For *NRP2* and *EPHB4*, on the y axis, expression levels are shown as a relative value to those in HUVECs. Data are presented as mean ± SD (n = 3). Statistically significant differences were evaluated using one-way ANOVA followed by Tukey's multiple comparison test. Groups that do not share the same letter above the plots differ significantly from each other ($p < 0.05$). The categorized p values are listed in Table S6. (H) NRP2 protein levels in $CD34^+$ cells were measured using flow cytometry. Data are presented as the mean of technical triplicates. undiff., undifferentiated.

expression of arterial markers (*C-X-C motif chemokine receptor 4* [*CXCR4*] and *ephrin B2* [*EFNB2*]) as well as of venous markers (*neuropilin2* [*NRP2*] and *EPH receptor B4* [*EPHB4*])[10–12] was evaluated by qPCR on day 6. Human umbilical artery endothelial cells (HUAECs) and HUVECs were used as arterial and venous control cells. As shown in Figure 3G, the expression of arterial markers (*CXCR4* and *EFNB2*) was lower in $CD34^+$ cells than in HUAECs. The expression of *EFNB2* in $CD34^+$ cells was similar to that in HUVECs, whereas the expression of *CXCR4* in $CD34^+$ cells was significantly higher than that in HUVECs. Regarding venous markers (*NRP2* and *EFNB2*), their expression in $CD34^+$ cells was higher than that in HUAECs, HUVECs, and undifferentiated human iPSCs. Next, we determined the protein levels of NRP2 in $CD34^+$ cells using flow cytometry analysis and found that approximately 52% of cells were $NRP2^+$ cells (Figure 3H). These results indicate that $CD34^+CD31^+$ cells with venous-like characteristics could be efficiently induced using our modified protocol.

Differentiation of human iPSC-derived LSEC-like cells secreting coagulation factor VIII

We further attempted to differentiate obtained human iPSC-derived LPCs into LSEC-like cells by treatment with 1.5 μM A-83-01 (transforming growth factor β [TGF-β] signal inhibitor) and 1 mM cyclic

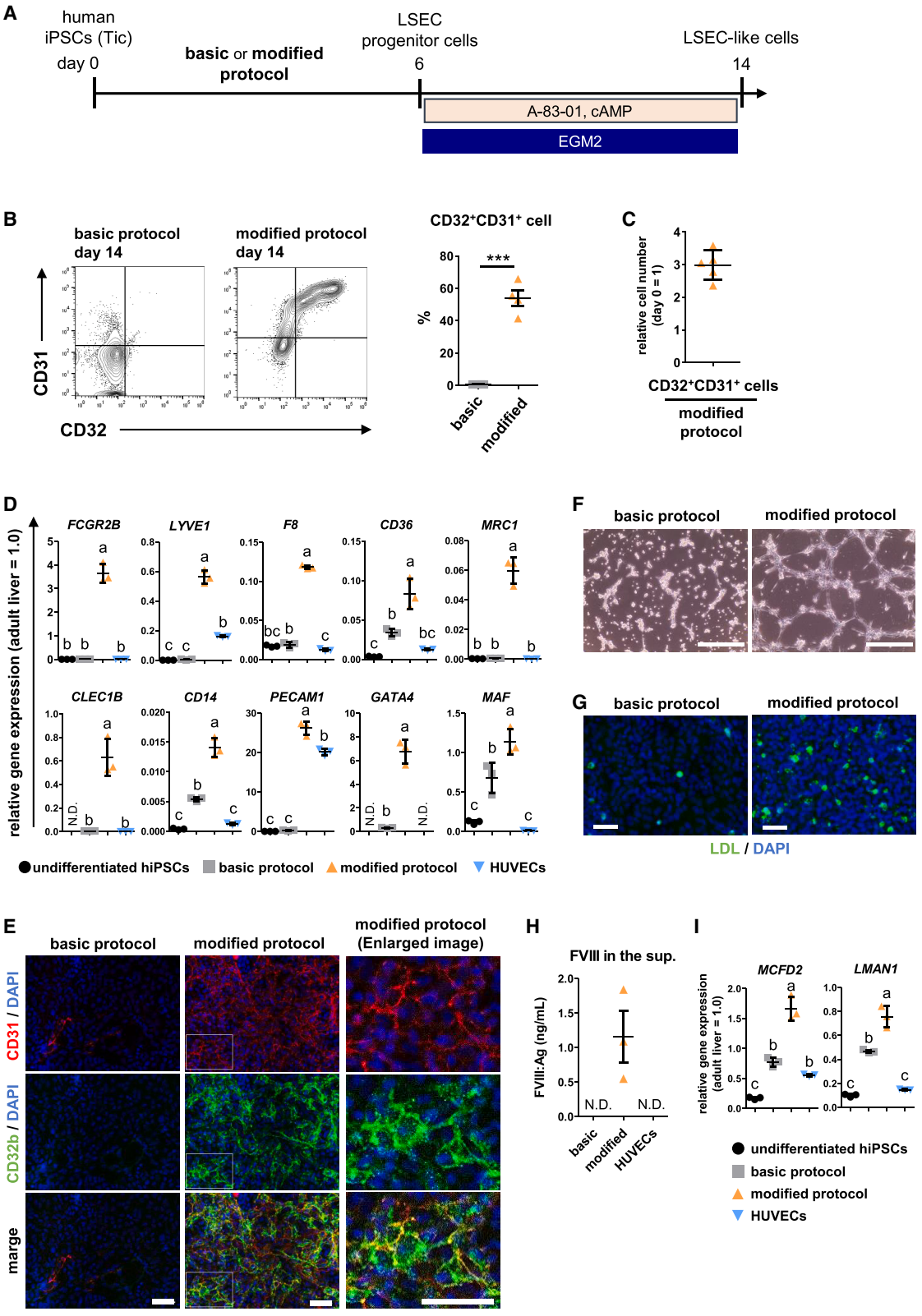

(legend on next page)

AMP (cAMP) with reference to previous reports.[5,6,13,14] As hypoxia promotes LSEC differentiation *in vitro*,[6] we used IOX2, a hypoxia-inducible factor prolyl-hydroxylase inhibitor, to mimic hypoxic culture conditions (Figure S2A). When we differentiated $CD34^+$ cells sorted using MACS into LSECs, IOX2 treatment significantly upregulated some LSEC-associated gene expressions (*Fc gamma receptor IIb* [*FCGR2B*], *coagulation factor 8* [*F8*], etc.) (Figure S2B). However, when we differentiated cells induced using the modified protocols without cell sorting and replating, cells were mostly dead following treatment with 25, 50, and 100 μM IOX2 (data not shown). Hence, in the case of LSEC differentiation induction without cell sorting and replating, we opted for normoxia culture conditions without IOX2 treatment. To evaluate the effect of basic medium on LSEC differentiation, differentiated cells induced using the modified protocol were differentiated into LSEC-like cells using EGM2 medium (an endothelial cell culture medium), B27/RPMI medium (a basic medium used for differentiation until LPCs), and their combination (Figure S3A). After differentiation, the percentages of LSEC-related marker-positive ($CD32^+$ and $CD31^+$) cells in the differentiated cells (day 14) were evaluated using flow cytometry analysis. Consequently, the percentage of CD32- and CD31-double positive cells in differentiated cells induced using EGM2 medium was higher than that using B27/RPMI medium alone (Figure S3B). The expression of LSEC-related genes (*FCGR2B*, *lymphatic vessel endothelial hyaluronan receptor 1* [*LYVE1*], *F8*, *CD36*) in human iPSC-derived cells induced using EGM2 medium was higher than that in cells induced using B27/RPMI medium alone (Figure S3C). Based on these results, we used EGM2 medium for LSEC differentiation in subsequent experiment (Figure 4A). To compare the efficiency of LSEC differentiation between the basic and modified protocols, we evaluated the percentage of LSEC-related marker-positive ($CD32^+$ and $CD31^+$) cells in differentiated cells (day 14) using flow cytometry (Figure 4B). The percentage of $CD32^+CD31^+$ cells in cells induced using the modified protocol was higher than that in cells induced using the basic protocol (approximately 54% vs. 0.5%). In addition, the total number of CD32- and CD31-double positive cells induced using the modified protocol at day 14 were approximately 3.0-fold greater than the initial number of cells at day 0 (Figure 4C).

The expression of LSEC-related genes (*FCGR2B*, *LYVE1*, *F8*, *CD36*, *mannose receptor C-type 1* [*MRC1*], *C-type lectin domain family 1 member B* [*CLEC1B*], also known as *CLEC2*, *CD14, PECAM1*, *GATA binding protein 4* [*GATA4*], and *MAF bZIP transcription factor* [*MAF*])[1,2,14–18] in human iPSC-derived cells induced using the modified protocol (day 14) were significantly higher than that in undifferentiated human iPSCs, human iPSC-derived cells induced using the basic protocol, and HUVECs (a non-liver-specific EC) (Figure 4D). Immunocytochemical analysis revealed $CD32b^+$ cells in human iPSC-derived cells induced using the modified protocol (day 14) (Figure 4E). To examine the functions of human iPSC-derived cells (day 14), we evaluated their tube formation and low-density lipoprotein (LDL) uptake capacity. Differentiated cells induced using the modified protocol demonstrated tube-like structures on Matrigel *in vitro* 6 h after seeding (Figure 4F). In addition, their LDL uptake was observed after culturing with medium containing Alexa Fluor 488-labeled acetylated LDL for 15 min (Figure 4G). To examine the FVIII secretion potency of human iPSC-derived cells, we analyzed the amount of FVIII antigen in the culture supernatant using enzyme-linked immunosorbent assay (ELISA). Substantial levels of human FVIII antigen were detected in the supernatant of human iPSC-derived cells induced using the modified protocol, but not in the supernatant of human iPSC-derived cells induced using the basic protocol, and HUVECs (Figure 4H). Furthermore, we examined the expression of *MCFD2* and *LMAN1*, which play an important role in intracellular trafficking and efficient secretion of FVIII.[19–21] Their expression in human iPSC-derived cells induced using the modified protocol were significantly higher than those in undifferentiated human iPSCs, human iPSC-derived cells induced using the basic protocol, and HUVECs (Figure 4I). These data suggest that our modified protocol efficiently induced FVIII-secreting LSEC-like cells from human iPSCs.

Figure 4. Characterization of human iPSC-derived cells after LSEC differentiation induction

(A) The schematic representation of the protocol for the differentiation of human iPSCs (Tic) into LSEC-like cells. (B) The percentage of $CD32^+CD31^+$ cells in human iPSC derivatives from the basic and the modified protocols was measured using flow cytometry analysis. Data are presented as mean ± SEM ($n = 4$, four independent experiments). Statistically significant differences were evaluated using an unpaired two-tailed Student's t test (***$p < 0.001$). (C) The number of $CD32^+CD31^+$ cells induced using the modified protocol relative to the total cell number at day 0. The number of $CD32^+CD31^+$ cells was calculated from the total cell number and the percentage of $CD32^+CD31^+$ cells measured using flow cytometry on day 14. On the y axis, the total cell number at day 0 taken as 1. Data are presented as mean ± SD ($n = 5$). (D) qPCR analysis of *FCGR2B*, *LYVE1*, *F8*, *CD36*, *MRC1*, *CLEC1B*, *CD14*, *PECAM1*, *GATA4*, and *MAF* expression in the undifferentiated human iPSCs, human iPSC derivatives from the basic and the modified differentiation protocols on day 14, and HUVECs. On the y axis, expression levels are shown as a relative value to those of the adult human liver tissue sample. Data are presented as mean ± SD ($n = 3$). Statistically significant differences were evaluated using one-way ANOVA followed by Tukey's multiple comparison test for multi-group comparisons or using an unpaired two-tailed Student's t test for two-group comparison. Groups that do not share the same letter above the plots differ significantly from each other ($p < 0.05$). The categorized p values were listed in Table S7. (E) Immunocytochemical analysis of CD32b (green) and CD31 (red) in human iPSC-derived cells from the basic and modified differentiation protocols (day 14). Nuclei were counterstained with DAPI (blue). Scale bars, 50 μm. (F) Analysis of tube formation on Matrigel capacity of iPSC-derived cells from the basic and the modified differentiation protocols on day 14. Scale bars, 500 μm. (G) Analysis of LDL uptake capacity of iPSC-derived cells from the basic and the modified differentiation protocols on day 14. Scale bars, 50 μm. (H) Amounts of FVIII antigen in the culture supernatant of human iPSC-derived cells (differentiations day 14–16), and HUVECs were determined by ELISA. Data are presented as mean ± SEM ($n = 3$, three independent experiments). (I) qPCR analysis of genes (*MCFD2* and *LMAN1*) expression in undifferentiated human iPSCs, human iPSC derivatives from the basic and the modified differentiation protocols on day 14, and HUVECs. On the y axis, expression levels are shown as a relative value to those of the adult human liver tissue sample. Data are presented as mean ± SD ($n = 3$). Statistically significant differences were evaluated using one-way ANOVA followed by Tukey's multiple comparison test. Groups that do not share the same letter above the plots are significantly different each other ($p < 0.05$). The categorized p values are listed in Table S7. undiff., undifferentiated; N.D., not detected; sup., supernatant.

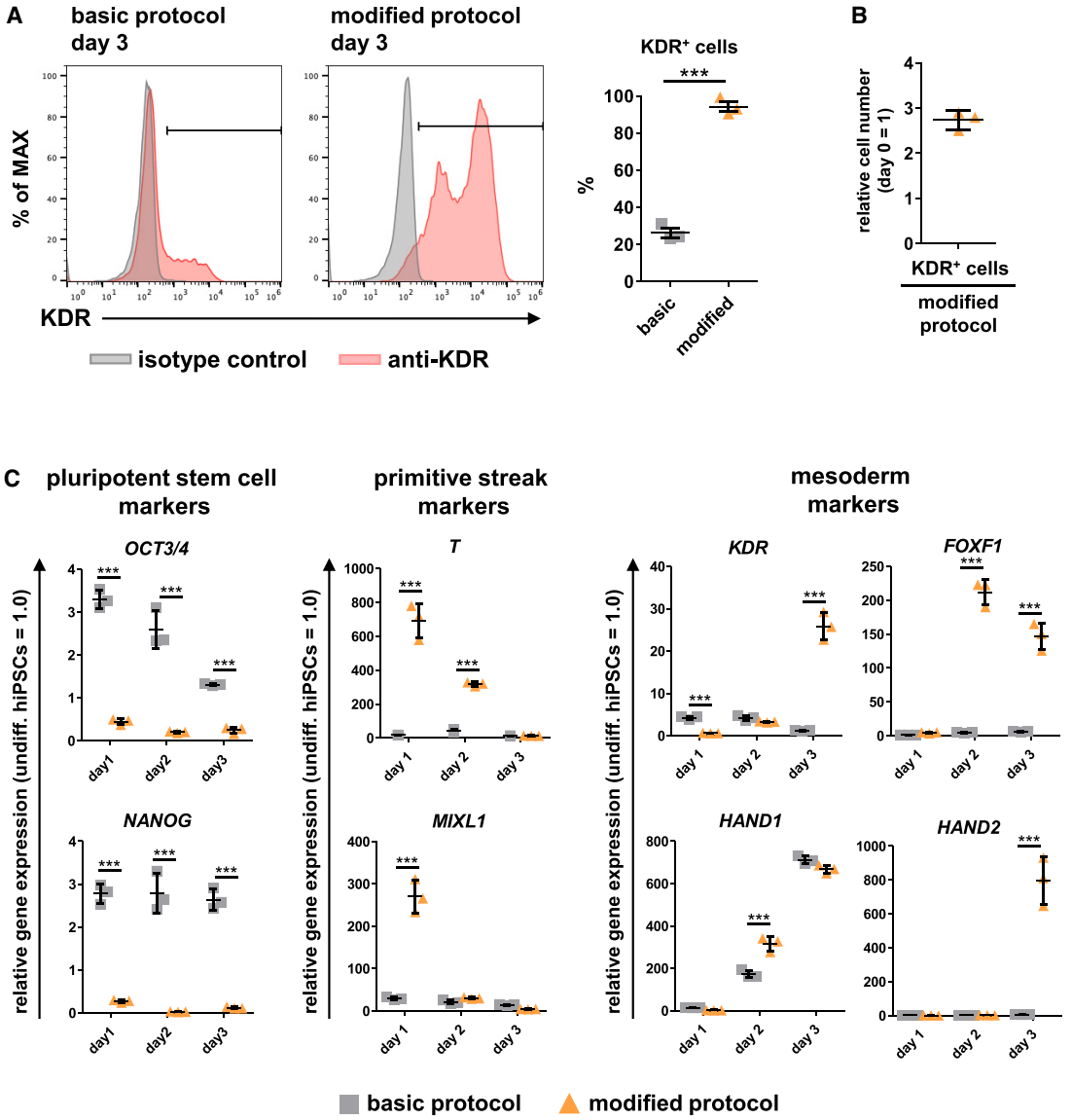

Figure 5. Evaluation of the modified differentiation protocol for the induction of KDR$^+$ mesoderm

(A) The percentage of KDR$^+$ cells in human iPSC derivatives was measured using flow cytometry analysis on day 3. Data are presented as mean ± SEM (n = 3, three independent experiments). Statistically significant differences were evaluated using an unpaired two-tailed Student's t test (***$p < 0.001$). (B) The number of KDR$^+$ cells induced using the modified protocol relative to the total cell number at day 0. The number of KDR$^+$ cells were calculated from the total cell number and the percentage of KDR$^+$ cells measured using flow cytometry on day 3. On the y axis, the total cell number at day 0 taken as 1. Data are presented as mean ± SD (n = 3). (C) qPCR analysis of *OCT3/4*, *NANOG*, *T*, *MIXL*, *KDR*, *FOXF1*, *HAND1*, and *HAND2* in human iPSC derivatives from the basic and the modified differentiation protocols (days 1–3). On the y axis, the expression levels are shown as a relative value to those of undifferentiated human iPSCs. Data are presented as mean ± SD (n = 3). Statistically significant differences were evaluated by two-way ANOVA followed by Bonferroni post-test (***$p < 0.001$).

Modified mesoderm induction method promoted KDR$^+$ mesoderm differentiation

We successfully established a mesoderm induction method to efficiently induce LPCs and LSEC-like cells. As kinase insert domain receptor (KDR, also known as VEGFR2, FLK1) positive mesoderm is one origin of endothelial-lineage cells,[22–24] we evaluated whether our modified protocol induced KDR$^+$ mesodermal cells from human iPSCs. The KDR$^+$ cell ratio in differentiated cells was examined using flow cytometry on day 3. Consequently, the percentage of KDR$^+$ cells in human iPSC-derived cells induced using the modified protocol was higher than that in cells induced using the basic protocol (approximately 94% vs. 26%) (Figure 5A). In addition, the total number of KDR$^+$ cells induced using the modified protocol at day 3 was approximately 2.7-fold greater than the

initial number of cells at day 0 (Figure 5B). Furthermore, we investigated the gene expression of pluripotent stem cell, primitive streak, and mesoderm markers in cells over time, up to differentiation day 3 (Figure 5C). For cells induced using the modified protocol, the expression of primitive streak markers (*T-box transcription factor T* [*T*, also known as *TBXT*], *Mix paired-like homeobox* [*MIXL1*])[25,26] peaked on day 1, whereafter the expression of mesoderm, especially the lateral plate mesoderm, related markers (*forkhead box F1* [*FOXF1*], *heart and neural crest derivatives expressed 1* [*HAND1*], and *heart and neural crest derivatives expressed 2* [*HAND2*])[24] peaked on days 2 and 3. The expression of most primitive streak and mesoderm markers in cells induced using the modified protocol was higher than in cells induced using the basic protocol. On the other hand, the gene expression of pluripotent stem cell markers (*OCT3/4*, also known as *POU class 5 homeobox 1* [*POU5F1*], and *NANOG*) in cells induced using the modified protocol was lower than that in cells induced using the basic protocol. These results indicate that our modified protocol could induce KDR$^+$ mesodermal cells more efficiently than the basic protocol.

LPCs and LSEC-like cells could be differentiated from different human iPSC lines using modified protocol

As it is known that there are variations between iPSC lines in terms of differentiation characteristics, we examined whether our modified protocol could induce LPCs and LSEC-like cells from different human iPSC lines. Another cell line of human iPSCs, called Dotcom, was differentiated into LPCs using the basic protocol and modified protocol, and then the percentage of their marker-positive cells was analyzed using flow cytometry analysis. Consequently, the percentage of CD34$^+$CD31$^+$ cells in cells induced using the modified protocol was higher than that in cells induced using the basic protocol at differentiation day 6 (Figure S4A). Next, we attempted to induce LSEC-like cells from the obtained differentiated cells (day 6) using the modified protocol. However, cell detachment was observed after medium change to EGM2 medium at differentiation day 6 (data not shown). To avoid this phenomenon, we used B27/RPMI medium as a basic medium between day 6 and 7 (Figure S4B). At differentiation day 14, the percentage of CD32$^+$CD31$^+$ cells in cells induced using the modified protocol was also significantly higher than that in cells induced using the basic protocol (Figure S4C). Furthermore, most of the LSEC-related gene expression in human iPSC-derived cells induced using the modified protocol was significantly higher than that in undifferentiated human iPSCs, human iPSC-derived cells induced using the basic protocol, and HUVECs (Figure S4D). These results indicated that LPCs and LSEC-like cells could be efficiently induced from different human iPSCs lines using the modified protocol.

DISCUSSION

In this study, we successfully developed an efficient method for the induction of LPCs and LSEC-like cells capable of secreting coagulation factor VIII *in vitro* from human iPSCs. This was achieved by optimizing the differentiation conditions of the mesoderm induction step.

At the optimal concentration and stimulation period with CHIR99021, BMP4, FGF2, and Activin A during the mesoderm induction step, on average approximately 65% and 54% of cells differentiated into LPCs and LSEC-like cells, respectively (Figures 3 and 4). One origin of endothelial cells is the KDR$^+$ mesoderm.[22–24] Our modified protocol efficiently induced KDR$^+$ mesoderm from human iPSCs through primitive streak differentiation. Meanwhile, cells subjected to the basic protocol potentially failed to exit from the pluripotent state during the mesoderm induction step (Figure 5). WNT/β-catenin signaling plays an important role in primitive streak formation.[27] Furthermore, there are multiple subtypes of mesoderm that are differentiated and characterized by the precise regulation of signaling pathways, such as WNT/β-catenin, BMP, and Activin/nodal signaling, *in vivo* and *in vitro*.[28–30] Although various differentiation methods for mesodermal cell induction have been reported, it is important to consider the specifics of *in vitro* differentiation induction protocols depending on the final cell type. Our results show that appropriate activation of WNT/β-catenin signaling via gradient treatment with CHIR99021 in the primitive streak and mesoderm induction step might be needed to efficiently promote the differentiation of human iPSCs into mesoderm which could subsequently differentiate into LPCs. However, although KDR$^+$ cells could be efficiently generated, the CD34$^+$CD31$^+$ cell ratio after LPC differentiation was relatively low. Thus, it is possible that heterogeneity may exist in the obtained KDR$^+$ cells in terms of their differentiation trajectories. Another possibility is that the method for LPC differentiation induction from mesoderm may require further improvement.

LPCs induced from mesoderm cells using our modified protocol could further differentiate into LSEC-like cells capable of secreting the FVIII protein *in vitro*. On average, the efficiency of LSEC-like cell induction was up to approximately 54% without cell purification throughout the entire differentiation induction process. Previous reports have indicated that hypoxia can promote LSEC differentiation from LPCs. Herein, when MACS-sorted CD34$^+$ cells were differentiated into LSECs, IOX2 treatment partially promoted LSEC differentiation (Figure S2). However, when we performed LSEC differentiation without cell sorting and replating, IOX2 treatment induced cell death (data not shown), whereas cells could differentiate into LSEC-like cells under normoxia culture conditions without IOX2 treatment. In the case of LSEC differentiation without cell purification, owing to the high cell density, an extreme hypoxic environment after IOX2 treatment might induce cell death. Transcription factor networks are central to cell differentiation and identity. The expression of GATA4 and MAF, key transcription factors involved in LSEC differentiation,[15,18] is believed to promote LSEC differentiation. The gene expression of *GATA4* and *MAF* in cells differentiated using our modified protocol was significantly higher than that in undifferentiated human iPSCs, cells differentiated using the basic protocol, and non-liver specific EC (HUVECs) (Figure 4D). Furthermore, MCFD2 and LMAN1 play important roles in the intracellular

trafficking of FVIII protein, and subjects with a defect in these genes exhibit decreased plasma FVIII levels, leading to a bleeding tendency.[19–21] In our experiment, the expression of *MCFD2*, *LMAN1*, and *F8* in human iPSC-derived cells induced using our modified protocol was significantly upregulated (Figures 4D and 4I). The expression of these factors might contribute to the acquisition of the LSEC-like phenotype and FVIII secretion capacity of differentiated cells. On the other hand, although IOX2 treatment upregulated some LSEC-related maker gene expression, *GATA4* and *MAF* were not upregulated (Figure S2B). This result indicates that other factors are also engaged in the LSEC differentiation process.

In this study, we designed the basic protocol for the induction of mesoderm and LPCs using a combination of cytokines as described previously.[4,6] However, the differentiation efficiency of KDR^+ cells (mesoderm) and $CD34^+CD31^+$ cells (LPCs) by the basic protocol were lower than expected. This phenomenon might be caused by differences other than the combination of cytokines, such as the cell culture dimensions. Mesoderm differentiation was performed under 3D culture conditions after EB formation in previous studies, whereas mesoderm differentiation was performed under 2D culture conditions in our study. In the case of our basic protocol, failure to differentiate into mesodermal cells caused subsequent LPC differentiation failure. Although the 3D culture condition (EB formation) might be essential to mesoderm induction in the published method,[4,6] we were able to significantly improve the differentiation induction efficiencies for $CD34^+$ and $CD31^+$ cells by modifying the mesoderm induction method in our study. This suggests that 3D culture is not required for the induction of mesoderm, a precursor of LPCs, from human iPSCs by using our established protocol. In addition, human iPSCs used in this study was maintained using StemFit AK02N and iMatrix-511-coated plate, and this method is different from that in previous reports.[4] The difference of undifferentiated human iPSC maintenance method affects their hepatic differentiation potency.[31] Since it is possible that the difference of human iPSC maintenance method also affect the mesoderm differentiation.

Through our method, approximately 4.8 $CD34^+CD31^+$ cells were generated from one human iPSC and this yield is higher than that reported previously (one input PSC generated 0.9 $CD34^+$ cells).[4] With respect to EB formation method, as cell proliferation was suppressed in the inner cells of EBs,[9] it is possible the total number of cells generated from one PSC in the published 3D method would be lower than that generated through our 2D method. The high yield of LPCs is particularly advantageous in the preparation of cell sources for hemophilia A cell therapy.

Our established protocol was considered adaptable to human iPSC lines other than those used herein, as multiple different human iPSC lines were differentiated into LPCs and LSEC-like cells more efficiently using the modified protocol than the basic protocol (Figures 3, 4, and S4). When we differentiated one human iPSC line (Dotcom) into LSEC-like cells, we observed partial cell detachment after medium change to EGM2. This phenomenon was not observed in the other human iPSC line (Tic). While the reason for this difference is unclear, this phenomenon could be avoided using B27/RPMI medium as the basic medium between differentiation day 6 and day 7, which gave rise to LSEC-like cells. Hence, no critical difference would exist in the characteristics of LPCs derived from different cell lines.

FVIII antigen was detected in the supernatant of human iPSC-derived LSEC-like cells, but we cannot ignore the potential contribution of FVIII released from dead cells. As notable cell death was not observed during differentiation days 14–16, we determined that human iPSC-derived LSEC-like cells could secrete FVIII. Although functional human iPSC-derived LSEC-like cells could be induced through our method, most of the LSEC-specific genes including *F8* were expressed at lower levels than in adult liver tissue containing LSECs (Figure 4D). Therefore, human iPSC-derived LSEC-like cells we developed were considered to still have an immature phenotype, indicating room for further modification of the LSEC induction method from LPCs. We previously reported that the cytokines related to liver development have important roles in the differentiation of LSEC-like cells from human bone marrow-derived mesenchymal stem cells.[32] These factors might have considerable influence on the maturation of human iPSC-derived LSEC-like cells.

In this study, there are several limitations to note. First, because the gene expression data were used to determine optimal protocol, the characteristics other than mRNA expression (e.g., protein synthesis and expression) were not considered in our decision. Second, as we hypothesized the heterogeneity in mesodermal cells induced using 3D method might cause low differentiation efficiency of LSEC and LPCs, we optimized a mesoderm induction method for LSEC differentiation. However, we did not perform analysis of the heterogeneity in mesodermal cells in this study, therefore the existence and effect of heterogeneity in mesodermal cells remains unclear. Finally, we could not perform the comparison of cells induced using our modified method and cells induced using published method directly. In our basic protocol, there are some differences from the published method, and our basic protocol failed to differentiate human iPSCs into LSEC progenitor and LSEC-like cells. Hence, the improvement from our basic protocol does not indicate advancement from the published method. Furthermore, the superiority of cells induced using our method as cell source for cell therapy (e.g., cell engraftment efficiency) is not clear. To show the utility of human iPSC derivatives induced using our method as cell source for cell therapy, cell transplantation experiments are necessary.

In conclusion, we established an *in vitro* induction method for LSEC-like cells capable of secreting FVIII from human iPSCs. We believe that these differentiated cells can be a promising cell source for allogeneic cell therapy of hemophilia A. As hemophilia A is a hereditary genetic disease, the developed LSEC differentiation protocol might also be useful for elucidating the characteristics of patient-specific genetic variants using iPSCs established from patients with hemophilia A. Moreover, LSECs play an important role in various liver diseases, including alcoholic liver disease and liver fibrosis.[33,34] Thus, we

believe that the method established herein will contribute to the development of new treatments not only for hemophilia A but also for various liver diseases.

MATERIALS AND METHODS

Materials

Total RNA of human adult liver tissue (pool of five donors) was purchased from BioChain (Newark, CA). A cell pellet of HUAECs was purchased from PromoCell (Heidelberg, Germany).

Cell culture

The human iPSC lines, Tic (JCRB1331; JCRB Cell Bank, Osaka, Japan) and Dotcom (JCRB1327; JCRB Cell Bank),[35] were purchased from JCRB Cell Bank and maintained in StemFit AK02N (Ajinomoto, Tokyo, Japan) on iMatrix-511 silk (Nippi, Osaka, Japan)-coated plates. HUVECs (Lonza, Basel, Switzerland) were purchased from Lonza and cultured in EGM2 (Lonza).

Differentiation of LSEC-like cells from human iPSCs

Human iPSCs were dissociated into single cells and plated on a Matrigel (Corning, Corning, NY)-coated plate (the thin-coating method). After confirming that cells reached 40%–70% confluence, differentiation induction was started. Differentiation was performed in three steps: (1) primitive streak and mesoderm differentiation, (2) LPC differentiation, and (3) LSEC-like cell differentiation.

Three different basic medium conditions were tested for primitive streak and mesoderm, and LPC differentiation. In condition I, RPMI 1640 (Sigma-Aldrich, St. Louis, MO) containing B27 Supplement Minus Vitamin A (0.5×) (Thermo Fisher Scientific, Waltham, MA), penicillin-streptomycin solution (1×) (Fujifilm, Osaka, Japan), and GlutaMAX supplement (1×) (Thermo Fisher Scientific) (referred to as "B27/RPMI medium") was used for primitive streak and mesoderm and LPC differentiation. In condition II, StemPro34 (Thermo Fisher Scientific) was used for primitive streak and mesoderm differentiation, and EGM2 was used for LPC differentiation. In condition III, StemPro34 (25%, v/v)/IMDM (75%, v/v, Thermo Fisher Scientific) containing ITS-X (1:10,000) (Thermo Fisher Scientific), penicillin-streptomycin solution (×1), 2 mM L-glutamine (Thermo Fisher Scientific), 50 μg/mL ascorbic acid (Sigma-Aldrich), 150 μg/mL transferrin (Roche), and 50 μg/mL monothioglycerol (Sigma-Aldrich) (referred to as "StemPro34/IMDM medium") was used for primitive streak and mesoderm, and LPC differentiation.

On day 0, for mesoderm differentiation, the human iPSC culture medium was replaced with B27/RPMI medium, StemPro34, or StemPro34/IMDM medium containing 0, 5, 10, or 15 μM CHIR99021 (GSK3 inhibitor; Cayman Chemical, Ann Arbor, MI), 0 or 12 ng/mL BMP4 (R&D Systems, Minneapolis, MN), 0 or 5 ng/mL FGF2 (Peprotech, Cranbury, NJ), and 0 or 4 ng/mL Activin A (R&D Systems). On day 1, the medium was changed to the respective medium containing 0, 2, 5, or 10 μM CHIR99021, 0 or 12 ng/mL BMP4, 0 or 5 ng/mL FGF2, and 0 or 4 ng/mL Activin A. On day 2, the medium was changed to the respective medium containing 0, 2, 5, or 10 μM CHIR99021, 12 ng/mL BMP4, 5 ng/mL FGF2, and 4 ng/mL Activin A.

For further differentiation into LPCs, differentiated mesodermal cells were cultured in B27/RPMI medium, EGM2, or StemPro34/IMDM medium containing 10 ng/mL vascular endothelial growth factor-A (VEGF-A) (Thermo Fisher Scientific), 10 ng/mL FGF2, and 10 μM DAPT (γ-secretase inhibitor; AdipoGen, San Diego, CA) for 3 days. On day 3 (the first day of LPC differentiation induction), all media in the wells were gently replaced with an LPC differentiation medium. On day 4, equal volumes of fresh differentiation medium was added to the culture wells without removing the old medium. On day 5, half of the medium in the culture well was removed and equal volumes of fresh media were gently added.

On day 6, for LSEC-like cell differentiation without cell sorting and replating, media were replaced with EGM2 or B27/RPMI medium containing 1.5 μM A-83-01 (TGF-β type I receptor inhibitor; Fujifilm), and 1 mM cAMP (8-bromoadenosine 3′,5′-cyclic monophosphate sodium salt, Sigma), then cultured for 8 days. During LSEC induction, the medium was changed at least once every 2 days.

When MACS-sorted $CD34^+$ cells were differentiated into LSEC-like cells, $CD34^+$ cells were plated on a Matrigel-coated plate (the thin-coating method) with EGM2 medium containing 1.5 μM A-83-01, 1 mM cAMP, and 0, 25, 50, or 100 μM IOX2 (Axon Medchem, Groningen, the Netherlands), and then cultured for 8 days. During LSEC induction, the medium was changed at least once every 2 days.

Preparation of $CD34^+$ cells

To purify $CD34^+$ cells from human iPSC-derived cells, CD34 MicroBead Kit, human (Miltenyi Biotec, Bergisch Gladbach, Germany), MiniMACS separator (Miltenyi Biotec), and MS columns (Miltenyi Biotec) were used. Cells were incubated with FcR Blocking reagent and CD34 MicroBeads at 4°C for 20 min. Cell suspension was then applied onto the column, and magnetically labeled cells were collected as $CD34^+$ cells. Collected $CD34^+$ cells were cryopreserved using CELLBANKER 1 (Nippon Zenyaku Kogyo, Koriyama, Japan).

Real-time PCR

To isolate the total RNA from cells, TRIzol Reagent (Thermo Fisher Scientific) was used. cDNA was synthesized from 500 ng total RNA using a High-Capacity RNA-to-cDNA kit (Thermo Fisher Scientific). Real-time PCR was performed with the Fast SYBR Green Master Mix (Thermo Fisher Scientific) using a StepOnePlus real-time PCR system (Thermo Fisher Scientific). Relative quantification of target mRNA levels was performed using the $2^{-(\Delta\Delta \text{ threshold cycle})}$ ($2^{-\Delta\Delta Ct}$) method. The values were normalized to those of the housekeeping gene, peptidylprolyl isomerase A (*PPIA*). The sequences of real-time PCR primers used in this study are listed in Table S1.

Flow cytometry

Cell suspensions of human iPSC derivatives were incubated with antibodies (listed in Table S2) at 4°C for 20 min. On differentiation

induction day 14, cell suspensions were incubated with Human TruStain FcX (Fc Receptor Blocking Solution) (BioLegend, San Diego, CA) before and during antibody incubation. After washing with 2% bovine serum albumin (BSA)/phosphate-buffered saline (PBS), flow cytometry was performed using a Spectral Analyzer SA3800 (Sony, Tokyo, Japan). Data analysis was performed using FlowJo software (Becton-Dickinson, Franklin Lakes, NJ).

Immunocytochemistry

Cells were fixed with methanol for 5 min at −20°C. Cells were treated with 0.1% Tween in PBS for 10 min at room temperature and then blocked with 10% FBS, 2% BSA, and 0.1% Tween 20 in PBS for 60 min at room temperature. Cells were incubated with the primary antibody (listed in Table S3) at 4°C overnight, and then with the secondary antibody (listed in Table S3) at room temperature for 1 h. Cells were stained with 4′,6-diamidino-2-phenylindole (DAPI) for 20 min and observed under a fluorescence microscope BZ-X710 (Keyence, Osaka, Japan).

Tube formation assay

Cells were seeded on a Matrigel-coated plate (the thick gel method). After 6 h, cells were observed using the EVOS XL core imaging system (Thermo Fisher Scientific).

Cellular uptake of LDL

Cells were cultured with EGM2 medium containing 10 μg/mL Alexa Fluor 488-labeled acetylated LDL (Thermo Fisher Scientific) for 15 min. After washing with PBS, the cells fixed with 4% paraformaldehyde for 10 min at room temperature. The cells were stained with DAPI for 20 min and observed under a fluorescence microscope BZ-X710 (Keyence).

ELISA

Culture supernatants were collected on day 16 after incubation for 48 h after the medium change, and the amount of human FVIII antigen in samples was quantified using a Matched-Pair Antibody Set for ELISA of human Factor VIII antigen (Affinity Biologicals, Ontario, Canada). Normal human plasma (Coagtrol N; Sysmex, Kobe, Japan) was used as the standard. The concentration of FVIII in Coagtrol N was set to 100 ng/mL.

Statistical analysis

Statistically significant differences were evaluated using one-way ANOVA followed by Tukey's multiple comparison test or two-way ANOVA followed by Bonferroni post-test for multi-group comparisons. For two-group comparison, statistically significant differences were evaluated with an unpaired two-tailed Student's t test. Statistical analysis was performed using GraphPad Prism software version 5 (GraphPad software, San Diego, CA).

DATA AND CODE AVAILABILITY

The data supporting the findings of this study are available from the corresponding author upon reasonable request.

ACKNOWLEDGMENTS

We would like to thank Editage (www.editage.com) for English language editing. This research was supported by the Japan Society for the Promotion of Science (JSPS) (KAKENHI grants 21K16008, 20H00531, and 24K18954), Bayer (Bayer Academic Support), Novo Nordisk (Novo Nordisk Access to Insight 2021 Basic Research Grant), and Terumo Life Science Foundation.

AUTHOR CONTRIBUTIONS

Conceptualization, S.M.; investigation, S.M., C.H., Y.O., and Y.T.; formal analysis, S.M. and C.H.; data curation, S.M. and C.H.; writing – original draft, S.M.; writing – review & editing, S.M., C.H., Y.O., Y.T., A.S., M.S., and K.T.; funding acquisition, S.M., M.S., and K.T.

DECLARATION OF INTERESTS

S.M. received grants from Bayer (Bayer Academic Support). K.T. received grants from Novo Nordisk (Novo Nordisk Access to Insight 2021 Basic Research Grant). A.S. received payment for lectures in the speaker's bureau from CSL Behring outside this study. M.S. received consultation fees from Chugai Pharmaceutical Co., Ltd.; research support (including funding) from Chugai Pharmaceutical Co., Ltd., Takeda Pharmaceutical Co., Ltd., and CSL Behring; and lectures in the speaker's bureau from Chugai Pharmaceutical Co., Ltd., Takeda Pharmaceutical Co., Ltd., and CSL Behring, Sanofi, Bayer, Novo Nordisk, Pfizer, and Fujimoto Seiyaku Corp. outside this study. All other authors declare no competing interests.

SUPPLEMENTAL INFORMATION

Supplemental information can be found online at https://doi.org/10.1016/j.omtm.2024.101355.

REFERENCES

1. Shahani, T., Covens, K., Lavend'homme, R., Jazouli, N., Sokal, E., Peerlinck, K., and Jacquemin, M. (2014). Human liver sinusoidal endothelial cells but not hepatocytes contain factor VIII. J. Thromb. Haemost. *12*, 36–42.
2. Hayakawa, M., Sakata, A., Hayakawa, H., Matsumoto, H., Hiramoto, T., Kashiwakura, Y., Baatartsogt, N., Fukushima, N., Sakata, Y., Suzuki-Inoue, K., and Ohmori, T. (2021). Characterization and visualization of murine coagulation factor VIII-producing cells in vivo. Sci. Rep. *11*, 14824.
3. Fomin, M.E., Zhou, Y., Beyer, A.I., Publicover, J., Baron, J.L., and Muench, M.O. (2013). Production of factor VIII by human liver sinusoidal endothelial cells transplanted in immunodeficient uPA mice. PLoS One *8*, e77255.
4. Gage, B.K., Merlin, S., Olgasi, C., Follenzi, A., and Keller, G.M. (2022). Therapeutic correction of hemophilia A by transplantation of hPSC-derived liver sinusoidal endothelial cell progenitors. Cell Rep. *39*, 110759.
5. Koui, Y., Kido, T., Ito, T., Oyama, H., Chen, S.-W., Katou, Y., Shirahige, K., and Miyajima, A. (2017). An In Vitro Human Liver Model by iPSC-Derived Parenchymal and Non-parenchymal Cells. Stem Cell Rep. *9*, 490–498.
6. Gage, B.K., Liu, J.C., Innes, B.T., MacParland, S.A., McGilvray, I.D., Bader, G.D., and Keller, G.M. (2020). Generation of Functional Liver Sinusoidal Endothelial Cells from Human Pluripotent Stem-Cell-Derived Venous Angioblasts. Cell Stem Cell *27*, 254–269.e9.
7. Sumi, T., Tsuneyoshi, N., Nakatsuji, N., and Suemori, H. (2008). Defining early lineage specification of human embryonic stem cells by the orchestrated balance of canonical Wnt/beta-catenin, Activin/Nodal and BMP signaling. Development *135*, 2969–2979.
8. Kreuser, U., Buchert, J., Haase, A., Richter, W., and Diederichs, S. (2020). Initial WNT/β-Catenin Activation Enhanced Mesoderm Commitment, Extracellular Matrix Expression, Cell Aggregation and Cartilage Tissue Yield From Induced Pluripotent Stem Cells. Front. Cell Dev. Biol. *8*, 581331.
9. Barzegari, A., Gueguen, V., Omidi, Y., Ostadrahimi, A., Nouri, M., and Pavon-Djavid, G. (2020). The role of Hippo signaling pathway and mechanotransduction in tuning embryoid body formation and differentiation. J. Cell. Physiol. *235*, 5072–5083.
10. Sriram, G., Tan, J.Y., Islam, I., Rufaihah, A.J., and Cao, T. (2015). Efficient differentiation of human embryonic stem cells to arterial and venous endothelial cells under feeder- and serum-free conditions. Stem Cell Res. Ther. *6*, 261.

11. Yamamizu, K., Matsunaga, T., Uosaki, H., Fukushima, H., Katayama, S., Hiraoka-Kanie, M., Mitani, K., and Yamashita, J.K. (2010). Convergence of Notch and beta-catenin signaling induces arterial fate in vascular progenitors. J. Cell Biol. *189*, 325–338.

12. Zhang, J., Chu, L.-F., Hou, Z., Schwartz, M.P., Hacker, T., Vickerman, V., Swanson, S., Leng, N., Nguyen, B.K., Elwell, A., et al. (2017). Functional characterization of human pluripotent stem cell-derived arterial endothelial cells. Proc. Natl. Acad. Sci. USA *114*, E6072–E6078.

13. Yoshida, M., Nishikawa, Y., Omori, Y., Yoshioka, T., Tokairin, T., McCourt, P., and Enomoto, K. (2007). Involvement of signaling of VEGF and TGF-beta in differentiation of sinusoidal endothelial cells during culture of fetal rat liver cells. Cell Tissue Res. *329*, 273–282.

14. Nonaka, H., Watabe, T., Saito, S., Miyazono, K., and Miyajima, A. (2008). Development of stabilin2+ endothelial cells from mouse embryonic stem cells by inhibition of TGFbeta/activin signaling. Biochem. Biophys. Res. Commun. *375*, 256–260.

15. Géraud, C., Koch, P.-S., Zierow, J., Klapproth, K., Busch, K., Olsavszky, V., Leibing, T., Demory, A., Ulbrich, F., Diett, M., et al. (2017). GATA4-dependent organ-specific endothelial differentiation controls liver development and embryonic hematopoiesis. J. Clin. Invest. *127*, 1099–1114.

16. Strauss, O., Phillips, A., Ruggiero, K., Bartlett, A., and Dunbar, P.R. (2017). Immunofluorescence identifies distinct subsets of endothelial cells in the human liver. Sci. Rep. *7*, 44356.

17. Su, T., Yang, Y., Lai, S., Jeong, J., Jung, Y., McConnell, M., Utsumi, T., and Iwakiri, Y. (2021). Single-Cell Transcriptomics Reveals Zone-Specific Alterations of Liver Sinusoidal Endothelial Cells in Cirrhosis. Cell. Mol. Gastroenterol. Hepatol. *11*, 1139–1161.

18. Gómez-Salinero, J.M., Izzo, F., Lin, Y., Houghton, S., Itkin, T., Geng, F., Bram, Y., Adelson, R.P., Lu, T.M., Inghirami, G., et al. (2022). Specification of fetal liver endothelial progenitors to functional zonated adult sinusoids requires c-Maf induction. Cell Stem Cell *29*, 593–609.e7.

19. Zheng, C., and Zhang, B. (2013). Combined deficiency of coagulation factors V and VIII: an update. Semin. Thromb. Hemost. *39*, 613–620.

20. Everett, L.A., Cleuren, A.C.A., Khoriaty, R.N., and Ginsburg, D. (2014). Murine coagulation factor VIII is synthesized in endothelial cells. Blood *123*, 3697–3705.

21. Zhu, M., Zheng, C., Wei, W., Everett, L., Ginsburg, D., and Zhang, B. (2018). Analysis of MCFD2- and LMAN1-deficient mice demonstrates distinct functions in vivo. Blood Adv. *2*, 1014–1021.

22. Shalaby, F., Ho, J., Stanford, W.L., Fischer, K.D., Schuh, A.C., Schwartz, L., Bernstein, A., and Rossant, J. (1997). A requirement for Flk1 in primitive and definitive hematopoiesis and vasculogenesis. Cell *89*, 981–990.

23. Sakurai, H., Era, T., Jakt, L.M., Okada, M., Nakai, S., Nishikawa, S., and Nishikawa, S.-I. (2006). In vitro modeling of paraxial and lateral mesoderm differentiation reveals early reversibility. Stem Cell. *24*, 575–586.

24. Prummel, K.D., Nieuwenhuize, S., and Mosimann, C. (2020). The lateral plate mesoderm. Development *147*, dev175059. https://doi.org/10.1242/dev.175059.

25. Kispert, A., and Herrmann, B.G. (1994). Immunohistochemical analysis of the Brachyury protein in wild-type and mutant mouse embryos. Dev. Biol. *161*, 179–193.

26. Pearce, J.J., and Evans, M.J. (1999). Mml, a mouse Mix-like gene expressed in the primitive streak. Mech. Dev. *87*, 189–192.

27. Marikawa, Y. (2006). Wnt/beta-catenin signaling and body plan formation in mouse embryos. Semin. Cell Dev. Biol. *17*, 175–184.

28. Wang, L., and Chen, Y.-G. (2016). Signaling Control of Differentiation of Embryonic Stem Cells toward Mesendoderm. J. Mol. Biol. *428*, 1409–1422.

29. James, R.G., and Schultheiss, T.M. (2005). Bmp signaling promotes intermediate mesoderm gene expression in a dose-dependent, cell-autonomous and translation-dependent manner. Dev. Biol. *288*, 113–125.

30. Tsujimoto, H., Kasahara, T., Sueta, S.-I., Araoka, T., Sakamoto, S., Okada, C., Mae, S.-I., Nakajima, T., Okamoto, N., Taura, D., et al. (2020). A Modular Differentiation System Maps Multiple Human Kidney Lineages from Pluripotent Stem Cells. Cell Rep. *31*, 107476.

31. Matoba, N., Yamashita, T., Takayama, K., Sakurai, F., and Mizuguchi, H. (2018). Optimal human iPS cell culture method for efficient hepatic differentiation. Differentiation. *104*, 13–21.

32. Mitani, S., Onodera, Y., Hosoda, C., Takabayashi, Y., Sakata, A., Shima, M., and Tatsumi, K. (2023). Generation of functional liver sinusoidal endothelial-like cells from human bone marrow-derived mesenchymal stem cells. Regen. Ther. *24*, 274–281.

33. Ding, B.-S., Cao, Z., Lis, R., Nolan, D.J., Guo, P., Simons, M., Penfold, M.E., Shido, K., Rabbany, S.Y., and Rafii, S. (2014). Divergent angiocrine signals from vascular niche balance liver regeneration and fibrosis. Nature *505*, 97–102.

34. Yang, Y., Sangwung, P., Kondo, R., Jung, Y., McConnell, M.J., Jeong, J., Utsumi, T., Sessa, W.C., and Iwakiri, Y. (2021). Alcohol-induced Hsp90 acetylation is a novel driver of liver sinusoidal endothelial dysfunction and alcohol-related liver disease. J. Hepatol. *75*, 377–386.

35. Nishino, K., Toyoda, M., Yamazaki-Inoue, M., Fukawatase, Y., Chikazawa, E., Sakaguchi, H., Akutsu, H., and Umezawa, A. (2011). DNA methylation dynamics in human induced pluripotent stem cells over time. PLoS Genet. *7*, e1002085.